Published in final edited form as:
J Magn Reson Imaging. 2013 March ; 37(3): 746–751. doi:10.1002/jmri.23810.

A Dedicated Automated Injection System for Dynamic Contrast-Enhanced MRI Experiments in Mice

Jan Sedlacik, PhD[1], **Adrianne Myers, MD**[2], **Ralf B. Loeffler, PhD**[1], **Regan F. Williams, MD**[3], **Andrew M. Davidoff, MD**[2], and **Claudia M. Hillenbrand, PhD**[1]

[1]Department of Radiological Sciences, St. Jude Children's Research Hospital, Memphis, TN

[2]Department of Surgery, St. Jude Children's Research Hospital, Memphis, TN

[3]Department of Surgery, University of Tennessee Health Science Center, Memphis, TN

Abstract

Purpose—To develop a reproducible small-animal dynamic contrast-enhanced (DCE) MRI set-up for mice through which volumes <100μL can be accurately and safely injected and to test this set-up via DCE measurements in resting muscle and tumor tissue.

Materials and Methods—The contrast agent (CA) injection system comprised 2 MR-compatible syringe pumps placed 50cm from the 7T magnet bore where the fringe field is about 40mT. Microbore tubing and T-connector, close to the injection site, minimized dead volume (<10μL). For DCE-MRI measurements in 8 CB-17 SCID mice with 1500–2500mm^3 large orthotopic neuroblastoma, a bolus of 10-fold-diluted Gd-DTPA CA solution (0.1mmol/kg) was delivered (5μL/s), followed by a 50μL saline flush. Retro-orbital injections were given instead of tail vein injections, since the peripheral vasculature was reduced because of large tumor burden.

Results—The CA injection was successful in 19 of 24 experiments. Optical assessment showed minimal dispersion of ink-colored CA bolus. Mean (±SD) pharmacokinetic parameters retrieved from DCE-MRI examinations in resting muscle (K^{trans}=0.038±0.025min^{-1}, k_{ep}=0.66±0.48min^{-1}, v_e=0.060±0.014, v_p=0.033±0.021) and tumor (K^{trans}=0.082±0.071min^{-1}, k_{ep}=0.82±0.80min^{-1}, v_e=0.121±0.075, v_p=0.093±0.051) agreed with those reported previously.

Conclusion—We successfully designed and implemented a DCE-MRI set-up system with short injection lines and low dead volume. The system can be used at any field strength with the syringe pumps placed at a sufficiently low fringe field (<40mT).

Keywords

mice; injection system; dynamic contrast enhanced MRI; arterial input function; retro-orbital

INTRODUCTION

Dynamic contrast-enhanced (DCE) MRI is a very useful tool for the early assessment of tumor angiogenesis and its response to therapy, as it noninvasively measures vascular function by using parameters such as blood flow and vessel permeability (1). Longitudinal measurements by DCE-MRI have been used to elucidate tumor vascular growth (2) and verify the effects of treatment, especially of antiangiogenic drugs, in preclinical small-animal models (3). Although MRI contrast delivery systems are commercially available and

Corresponding Author: Claudia Hillenbrand, St. Jude Children's Research Hospital, 262 Danny Thomas Place, Mail Stop 220, Memphis, TN 38105, USA, Tel: (901) 595-4118, Fax: (901) 595-3981, claudia.hillenbrand@stjude.org.

applicable for DCE-MRI in humans, the method remains to be standardized in small animals, and details of the contrast agent (CA) injection system and tubing as well as injection volumes and rates need to be comprehensively documented.

As injection volume, injection rate, and CA concentration can influence the accuracy and precision of DCE-MRI (4), a precise and reproducible experimental set-up is necessary to accurately conduct DCE-MRI experiments in small animals. It is especially challenging to design and construct such a DCE-MRI set-up in mice, because only a very small total injection volume (<100 μL) can safely be injected into mice at one time (5). Commercially available injection systems currently used in clinical MRI settings are not suitable for small animals, since they are optimized for high-pressure, high-volume injections (e.g., 15 mL in 1–3 s) (6). Therefore, in small animals, contrast agent (CA) injections are usually given manually or by custom-built single-pump injection systems. The details of such injection systems (e.g., used tubing, injection volumes and rates) are not well standardized or documented. In this study, we developed a DCE-MRI set-up for mice and tested it by measuring pharmacokinetic parameters in normal-appearing resting muscle and tumor tissues.

MATERIALS AND METHODS

Injection system and experimental DCE set-up

The CA injection system consisted of 2 MRI-compatible syringe pumps (Model 70–2130, Harvard Apparatus, Holliston, MA) placed 50 cm from the opening of the MRI bore (7 T, ClinScan, Bruker Biospin, Germany). At this distance the fringe field of the 7T ClinScan magnet is about 40 mT. For different magnet designs and/or higher field strengths the distance between the pumps and the magnet bore may have to be adapted. The pumps were loaded with 1 mL plastic syringes, one containing saline and the other containing 10-fold diluted gadopentetic acid (0.5 molar, Gd-DTPA, Magnevist; Berlex Laboratories, Wayne, NJ). The syringes were connected with a Tygon microbore tubing 130 cm in length (Cole Parmer, Vernon Hills, IL) [inner diameter (ID)/outer diameter (OD) = 0.76/2.29 mm] to a nonmagnetic stainless steel T-connector (Cole Parmer) (ID/OD = 0.58/0.90 mm), which was joined to a thinner Tygon tubing 15 cm in length (ID/OD = 0.25/0.76mm) by using a 1-cm-long piece of the thicker tubing as a coupling sleeve. The blunt end of a 27 G butterfly needle was connected to the end of the thin tubing. The dead volume from the T-connector to the tip of the needle was approximately 10 μL. Since the T-connector had no active component (e.g., valve) to separate and to switch between the saline and CA solution, the performance of the injection system and the quality of the contrast bolus were evaluated by using a CA solution colored with blue ink. The injection process was assessed optically by taking a sequence of digital photographs (Fig. 1a). The outflow solution was collected as 10 μL aliquots on equally sized blotting paper sheets (2×2 cm^2). The mean color intensity of the sheets was measured by using the ImageJ software (Wayne Rasband, US National Institutes of Health, Bethesda, MD). Uniformly illuminated digital photographs of all sheets were color inverted; region of interest (ROI) areas of 2×2 cm^2 completely enclosing each blot were used for measurement. This approach ensured that the actual blot size and color intensity contribute to the mean color intensity of the measured sheet. The relative CA concentration was calculated by linearly scaling the mean color intensity of each sheet between the average value of the 4 highest color intensities and the lowest color intensity of the blank sheet.

Before each DCE-MRI session, the entire injection line was gas-sterilized and filled first with the CA solution up to the T-junction and then to the end (i.e., the butterfly needle tip) with saline through the other line. A retro-orbital injection site was chosen for the mice, since they exhibited a large tumor burden at later time points with reduced peripheral blood

supply, i.e., collapsed tail veins, which did not allow reliable DCE-MRI measurements from tail-vein injections, as found in pilot experiments. The retro-orbital injections were carefully administered (7), because adverse effects are potentially hazardous to animals. To aid the retro-orbital injection, the mouse was positioned tail-first in the magnet. A custom-made nose piece, cut from Plexiglas, allowed safe fixation of the mouse in the MRI bed in tail-first position, delivery of gas mixture for anesthesia (2.0%–3.5% isoflurane in a 2.5 L/min O_2 flow), and placement of the needle at the correct angle and position for the retro-orbital injection (Fig. 2). When multiple animals were measured consecutively in a single session, only the 27 G butterfly needle needed to be replaced with a new sterile needle; the rest of the injection system remained unchanged. Also, the feeding injection lines stayed filled and sterile, significantly reducing set-up times.

For DCE-MRI measurements, a single dose of CA (0.1 mmol/kg), corresponding to 50 μL of a 10-fold-diluted CA for a mouse weighing 25 g, was injected at the twentieth acquisition of the dynamic imaging sequence and immediately flushed with 50 μL of saline. The injection speed of both pumps was 5 μL/s, yielding a total injection time of 20 s. If dispersion of the injection system is neglected, the CA bolus duration should be approximately 10 s, which is short enough to allow accurate DCE-MRI evaluation (4). The dynamic imaging sequence was repeated 300 times, which took approximately 18 min. Respiration rate and body temperature were monitored by a small-animal monitoring system (Model 1025, SA Instruments, Inc., Stony Brook, NY). The temperature was maintained by a water circulation system integrated into the standard mouse bed of the MR-system. During the DCE experiment, the individual body temperature of animals was kept stable within a range of 1–2°C. The average body temperature of the animals ranged from 30°C to 37°C, and the respiration rates ranged from 30 to 40 min^{-1}. To minimize motion during MRI, the scanned body section of the mouse was properly fixed by taping this region to the mouse bed while taking care to not suppress the animal's respiration in general.

Animals and tumor model

Orthotopic neuroblastoma xenografts were established in 8 severe combined immunodeficient (SCID) mice. Three weeks after retroperitoneal neuroblastoma (NB1691) tumor cell inoculation, tumors were approximately 100 mm^3 in size and the longitudinal DCE-MRI study was initiated. Four mice served as controls and two each were treated with continuous delivery of interferon-beta (8) and single-dose bevacizumab (9). Both agents target the tumor vasculature by causing anti-angiogenesis, which controls tumor growth and size (8,9). After obtaining a baseline MRI, 2 follow-up DCE-MRIs were obtained for each mouse at different time points between day 2 and 11. Multiple follow-up time points and treatment groups were chosen to confirm the reproducibility of our DCE-MRI set-up under different experimental conditions. In total, 24 DCE-MRI examinations were performed. All animal experiments were performed in accordance with guidelines of the Animal Care and Use Committee.

MRI and data evaluation

Nonselective saturation recovery (SR) FLASH images (10), velocity-compensated in slice selection direction, were acquired on a 7 T small-animal MRI scanner (ClinScan, Bruker Biospin, Germany). Magnetization recovery was measured in a single shot (snapshot) by 16 inversion time points with TI = 82–3344.5 ms, ΔTI = 217.5 ms, TE = 1.53 ms, echo spacing = 2.7 ms, TR = 3562 ms, flip angle (FA) = 5°, acquisition matrix 128 × 80, field of view (FoV) 32 × 27 mm^2, 6/8 partial Fourier, and bandwidth = 550 Hz/pixel, yielding a spatial and temporal resolution of approximately 0.25 × 0.34 × 1 mm^3 and 3.5 s, respectively. Since the snapshot SR-FLASH sequence measures only an effective spin-lattice relaxation rate R_1*, relaxivity of the CA was calibrated by using a phantom with different aqueous

solutions of Gd-DTPA (0.1, 0.2, 0.3, 0.4 mM) measured at different temperatures (27°C–37°C, in increments of 1°C). The R_1*- and temperature-calibrated effective relaxivity (r_1*) was

$$r_1 * = 6.11\,(\mathrm{mM}\cdot\mathrm{s})^{-1} - 0.076\cdot T[^{\circ}\mathrm{C}]\,(\mathrm{mM}\cdot\mathrm{s}\cdot{}^{\circ}\mathrm{C})^{-1}, \quad [1]$$

where T is the temperature (°C). By solving Eq. 1, the effective relaxivity of Magnevist at 7 T and 37°C was found to be 3.30 $(\mathrm{mM}\cdot\mathrm{s})^{-1}$.

The dynamically measured R_1* values were converted to ΔR_1*, with the average native R_1* of the first 20 scans serving as baseline. The ΔR_1* was then converted to CA concentration by using the temperature-calibrated effective relaxivity (Eq. 1). The generalized two-compartment kinetic model (11) was fitted to the DCE curves by

$$C_t(t) = K^{\mathrm{trans}} \cdot C_p(t) \otimes \exp(-k_{ep}\cdot t) + v_p \cdot C_p(t), \quad [2]$$

where C_t and C_p are tissue and plasma concentration of the agent, respectively; v_p the fractional plasma volume; K^{trans} the transfer constant; and k_{ep} the rate constant, with

$$k_{ep} = K^{\mathrm{trans}}/v_e, \quad [3]$$

where v_e denotes the fractional interstitial space. $C_p(t)$ was estimated for each mouse individually by a tri-exponential fit from the vascular input function of the aorta (C_a), corrected by the hematocrit (*hct*) with

$$C_p(t) = C_a(t)/(1-hct), \quad [4]$$

with the *hct* assumed to be 0.45 (12). MatLab 7.6 (MathWorks, Inc., Natick, MA) was used for DCE data processing. A tri-exponential function was chosen to fit the AIF for individual DCE analysis because the 3-compartment open model is most appropriate to describe the blood plasma kinetics of Gd-DTPA in small animals (13). ROI-based analysis were identified on pharmacokinetic parameters maps and verified by realigned anatomic image slices (Fig. 3).

RESULTS

Optical inspection of the injection process and quantitative analysis with ImageJ revealed that the contrast bolus was formed regularly, with a duration of 11.2 s, steep slopes, and only 2.5% residual CA left after the saline flush (Fig. 1b).

The CA injection failed in 5 DCE experiments (failure rate 20.8%), leaving 19 datasets for processing and analysis. Figure 4 shows arterial input function (AIF) values obtained from the remaining 19 DCE experiments, the median AIF(t) $(0.57\cdot e^{-1.49\cdot t} \cdot 0.59\cdot e^{-0.086\cdot t})$ fitted bi-exponetially for better comparison to previously reported AIFs in mice acquired with similar CA injection settings (14). Table 1 compares the mean values (± standard deviation) of all pharmacokinetic parameters of the muscle and tumor tissue obtained from our DCE-MRI studies with those from previously reported small-animal DCE-MRI studies of muscle (15,16,17) and tumor (14) regions.

DISCUSSION

As the technical details of small-animal DCE-MRI experiments have not been clearly reported in literature, we designed and tested an experimental set-up for consecutive DCE-MRI measurements in tumor-bearing mice. We also report the DCE-MRI measures of normal-appearing resting muscle tissue and orthotopic neuroblastoma tumor xenografts. The CA injection system had short injection lines and a low dead volume, enabling the injection of a sharp bolus with very small volume, which is especially crucial for mice. Mice weighting about 25g have a total blood volume of approximately 1mL, and only injection volumes less than an additional 10% of this volume (100 μL) are considered safe (5). Furthermore, large injection volumes may considerably increase the animal's total blood volume, which could potentially compromise the results of the DCE measurement.

The rate of failed CA injections (20.8%) was relatively high, and injections failed randomly among animals and over time due to minor technical problems such as improperly loaded syringe pumps, pinched injection lines, or a clogged injection needle, but not because of the experimental design. We have revised our DCE-MRI protocol and currently inject 2 μL of saline every 2 min after placing the needle and before starting the DCE experiment. This simulates a drip infusion to maintain venous flow and successfully prevents clogging of the injection needle. Alternatively, very-low-dose heparin (10 units/mL) can be used in the injection solution to achieve the same effect (18). At present, for various other studies, we routinely use the presented injection system for pre/post-CA T1w imaging and its success rate is now more than 90%. Retro-orbital injection has been reported an effective route to administer radioactive tracers for PET imaging (19) or microbubble contrast agents for ultrasonography (20) in mice. For our study, we chose the retro-orbital injection because pilot experiments with the same tumor mouse model showed that many tail vein injections failed, especially at later time points with progressed disease. The frequent observation of collapsed tail veins may be specific to our orthotopic tumor model where the tumor grows inside the body directly next to the kidney, abdominal aorta and vena cava. Therefore, smaller sized tumors may have much more severe paraneoplastic effects than, e.g., subcutaneously grown tumors. However, the DCE-MRI set-up proposed in our study is not dependent on a particular injection site and tail vein injections may work just fine for other tumor models.

AIF, muscle, and tumor measurements from our DEC-MRI set-up are in agreement with those reported in other small-animal DCE-MRI studies (14,15,16,17). However, previously reported results of DCE-MRI in tumor tissues are highly variable and strongly depend on the tumor type and heterogeneity (21).

The dynamic imaging protocol used in our study was intended to enable direct measurements of relaxation rates by using snapshot-FLASH (10). This sequence does not need an additional T1 map measurement otherwise necessary to adjust the signal of conventional T1-weighted dynamic images. To improve temporal resolution and allow reliable measurements of the AIF, a global saturation pulse and velocity compensating gradients in the slice direction were used with the snapshot-FLASH sequence. It is important to choose a sufficient high resolution and large arteries to avoid partial volume effects in the AIF. We acquired our DCE-MRI data with a 0.25 × 0.34 × 1 mm3 voxel size and choose the abdominal aorta for defining the AIF, which is about 0.5–1mm in diameter and several mm in length; therefore, we are certain to have excluded potential partial volume effects. The use of a saturation pulse instead of an inversion pulse limits the ability to correct the measured effective spin-lattice relaxation rate (R_1*) for saturation effects due to RF pulses of the FLASH imaging. This limitation, however, was circumvented by calibrating the sequence for R_1* and temperature (Eq. 1) with quantitative phantom measurements. Another

limitation of the global nature of the saturation or inversion pulses is that only a single slice can be imaged. However, because the same anatomical slice can almost always be imaged, major blood vessels and the back muscle region can be reliably found, although tumor regions may differ between different exams. Future studies investigating heterogeneous tumors can use alternative methods capable of multislice or 3D dynamic imaging in order to obtain a more comprehensive view of the tumor, its growth patterns, and treatment response.

In conclusion, the developed small animal injection system is feasible for MR-DCE measurements in tumor bearing mice where low injection volumes are very critical. The automated injection system also offers the possibility to standardize the injection protocol which may help to decrease the variability of the obtained pharmacokinetic parameters, which in turn may reduce the minimal number of animals necessary for evident studies. The injection system is independent of the MR scanner and can therefore be used universally, also at different MR field strengths and bore sizes; if needed, the tubing can be scaled to accommodate larger-sized animals.

Acknowledgments

This study was supported by the American Lebanese Syrian Associated Charities (ALSAC) and in part by the United States Public Health Service Cancer Center Support Program Project Grant CA023099. The authors thank Melissa Johnson, Ziwei Zhang, and Chris Calabrese from the Small Animal Imaging Center at St. Jude for their assistance in DCE data acquisition; Adam Winchell from the Department of Radiological Sciences at St. Jude for technical assistance with the experimental DCE set-up; Axel Krafft from the Department of Radiological Sciences at St. Jude for critical review; and David Galloway and Vani Shanker from the Department of Scientific Editing at St. Jude for assistance with editorial review.

References

1. Barrett T, Brechbiel M, Bernardo M, Choyke PL. MRI of tumor angiogenesis. JMRI. 2007; 26(2): 235–249. [PubMed: 17623889]
2. Veeravagu A, Hou LC, Hsu AR, et al. The temporal correlation of dynamic contrast-enhanced magnetic resonance imaging with tumor angiogenesis in a murine glioblastoma model. Neurol Res. 2008; 30(9):952–959. [PubMed: 18662497]
3. Gossmann A, Helbich TH, Kuriyama N, et al. Dynamic contrast-enhanced magnetic resonance imaging as a surrogate marker of tumor response to anti-angiogenic therapy in a xenograft model of glioblastoma multiforme. JMRI. 2002; 15(3):233–240. [PubMed: 11891967]
4. Aerts HJ, van Riel NA, Backes WH. System identification theory in pharmacokinetic modeling of dynamic contrast-enhanced MRI: influence of contrast injection. MRM. 2008; 59(5):1111–1119.
5. Donovan, J.; Brown, P. Parenteral injections. In: Coligan, John E., et al., editors. Current protocols in immunology. Vol. Chapter 1. 2006. p. 6
6. Brummett D, Fidler J, Stark D. Power injectors for MRI. Applied Radiol. 1999; 28(5):16–20.
7. Yardeni T, Eckhaus M, Morris HD, Huizing M, Hoogstraten-Miller S. Retro-orbital injections in mice. Lab Anim. 2011; 40(5):155–160.
8. Dickson PV, Hamner JB, Streck CJ, et al. Continuous delivery of IFN-beta promotes sustained maturation of intratumoral vasculature. Mol Cancer Res. 2007; 5(6):531–542. [PubMed: 17579115]
9. Dickson PV, Hamner JB, Sims TL, et al. Bevacizumab-induced transient remodeling of the vasculature in neuroblastoma xenografts results in improved delivery and efficacy of systemically administered chemotherapy. Clin Cancer Res. 2007; 13(13):3942–3950. [PubMed: 17606728]
10. Frahm J, Haase A, Matthaei D. Rapid NMR imaging of dynamic processes using the FLASH technique. MRM. 1986; 3(2):321–327.
11. Tofts PS, Brix G, Buckley DL, et al. Estimating kinetic parameters from dynamic contrast-enhanced T(1)-weighted MRI of a diffusable tracer: standardized quantities and symbols. JMRI. 1999; 10(3):223–232. [PubMed: 10508281]

12. Daga A, Muraglia A, Quarto R, Cancedda R, Corte G. Enhanced engraftment of EPO-transduced human bone marrow stromal cells transplanted in a 3D matrix in non-conditioned NOD/SCID mice. Gene Ther. 2002; 9(14):915–921. [PubMed: 12085239]

13. Wedeking P, Eaton S, Covell DG, Nair S, Tweedle MF, Eckelman WC. Pharmacokinetic analysis of blood distribution of intravenously administered 153Gd-labeled Gd(DTPA)2-and 99mTc(DTPA) in rats. Magn Reson Imaging. 1990; 8(5):567–575. [PubMed: 2082126]

14. Weidensteiner C, Rausch M, McSheehy PM, Allegrini PR. Quantitative dynamic contrast-enhanced MRI in tumor-bearing rats and mice with inversion recovery TrueFISP and two contrast agents at 4.7 T. JMRI. 2006; 24(3):646–656. [PubMed: 16878308]

15. Faranesh AZ, Kraitchman DL, McVeigh ER. Measurement of kinetic parameters in skeletal muscle by magnetic resonance imaging with an intravascular agent. MRM. 2006; 55(5):1114–1123.

16. Yankeelov TE, DeBusk LM, Billheimer DD, et al. Repeatability of a reference region model for analysis of murine DCE-MRI data at 7T. JMRI. 2006; 24(5):1140–1147. [PubMed: 17024660]

17. Donahue KM, Weisskoff RM, Parmelee DJ, et al. Dynamic Gd-DTPA enhanced MRI measurement of tissue cell volume fraction. MRM. 1995; 34(3):423–432.

18. Wu X, Jeong EK, Emerson L, Hoffman J, Parker DL, Lu ZR. Noninvasive evaluation of antiangiogenic effect in a mouse tumor model by DCE-MRI with Gd-DTPA cystamine copolymers. Mol Pharm. 2010; 7(1):41–48. [PubMed: 19958031]

19. Nanni C, Pettinato C, Ambrosini V, et al. Retro-orbital injection is an effective route for radiopharmaceutical administration in mice during small-animal PET studies. Nucl Med Commun. 2007; 28(7):547–553. [PubMed: 17538396]

20. Miller DL, Dou C. Contrast-aided diagnostic ultrasound does not enhance lung metastasis in a mouse melanoma tumor model. J Ultrasound Med. 2005; 24(3):349–354. [PubMed: 15723847]

21. Alic L, van Vliet M, van Dijke CF, Eggermont AM, Veenland JF, Niessen WJ. Heterogeneity in DCE-MRI parametric maps: a biomarker for treatment response? Phys Med Biol. 2011; 56(6): 1601–1616. [PubMed: 21335648]

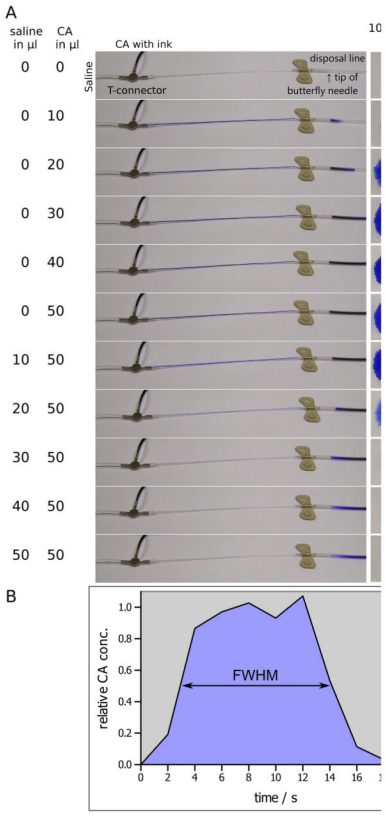

Figure 1.

A: Optical assessment of a contrast agent (CA) bolus injection in increments of 10 μL. The 2 left columns denote the cumulative amount of injected saline and ink-colored CA solution. The center column shows the flow of the contrast agent from the T-connector to the tip of the butterfly needle into a disposal line. The column right of the center column shows blots of 10 μL drops in which color intensities were used to estimate relative CA concentrations of the bolus (far right column) with respect to the average concentration of the 4 highest CA concentrations. **B:** Graphical representation of the CA-bolus. The full width at half-maximum (FWHM) represents the bolus length, which was approximately 10 s.

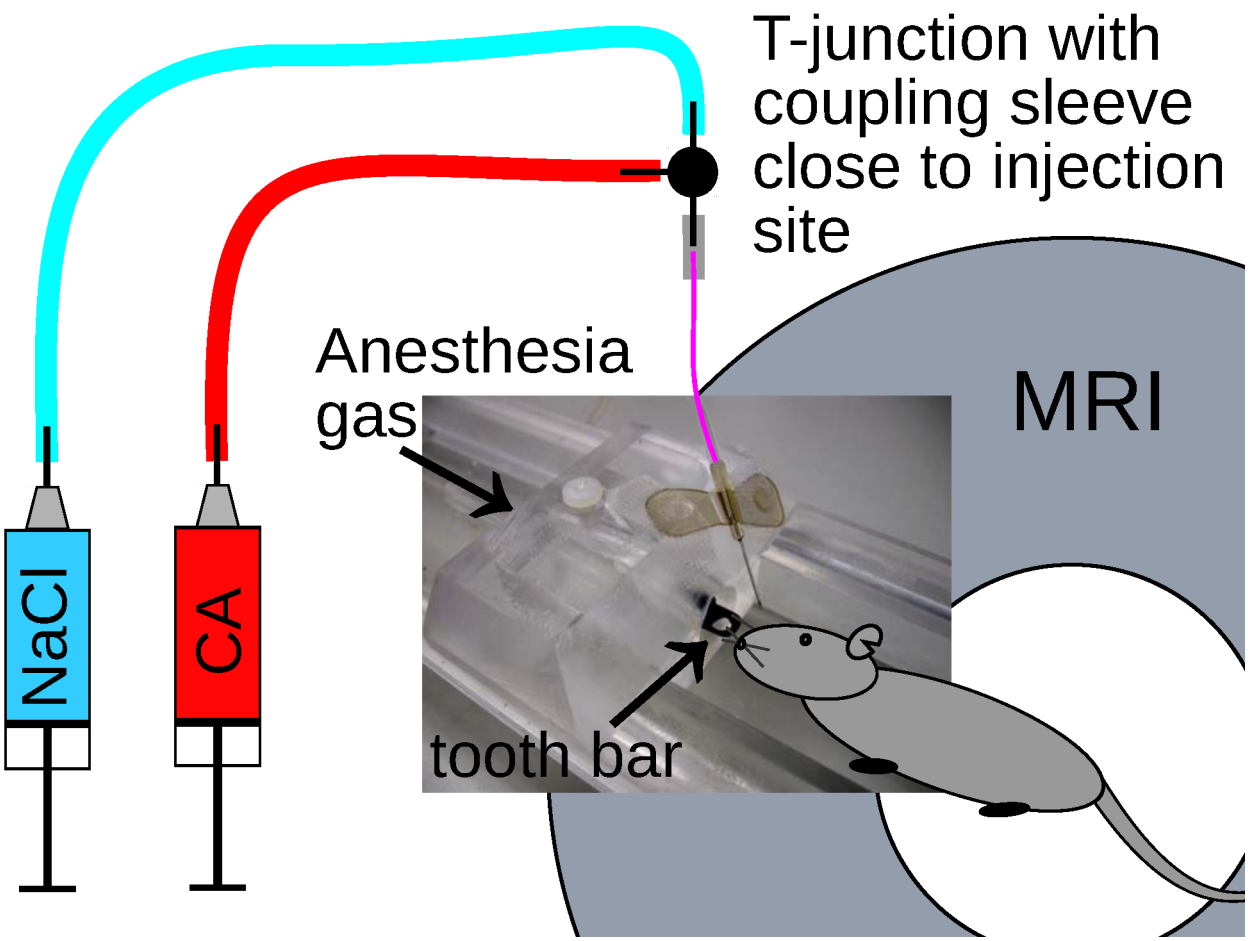

Figure 2.
Scheme of the injection system with a custom-made nose piece cut from Plexiglas, which sat tightly in the standard mouse bed of the MR-system; anesthesia was delivered through the plastic tube with a tooth bar. The tapered rim of the nose piece allowed fixing of the 27 G butterfly needle at the correct angle and position for retro-orbital injection.

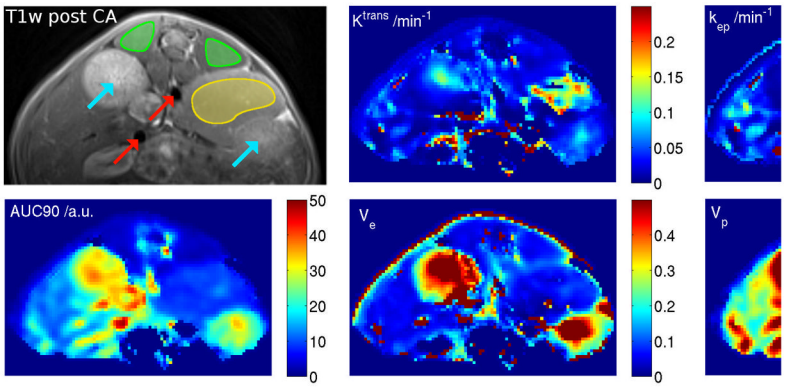

Figure 3.

Anatomic slice and corresponding maps of pharmacological parameters (AUC90, K^{trans}, k_{ep}, v_e and v_p). Pixels for arterial input function (AIF) estimation and regions of interest (ROIs) for DCE-MRI evaluation were selected on the AUC90 map. Anatomic confirmation ensured that only large vessels were used for AIF derivation (red arrows) and for DCE-MRI evaluation muscle (green ROIs) and tumor (yellow ROIs) was used. Turquoise arrows denote the kidneys.

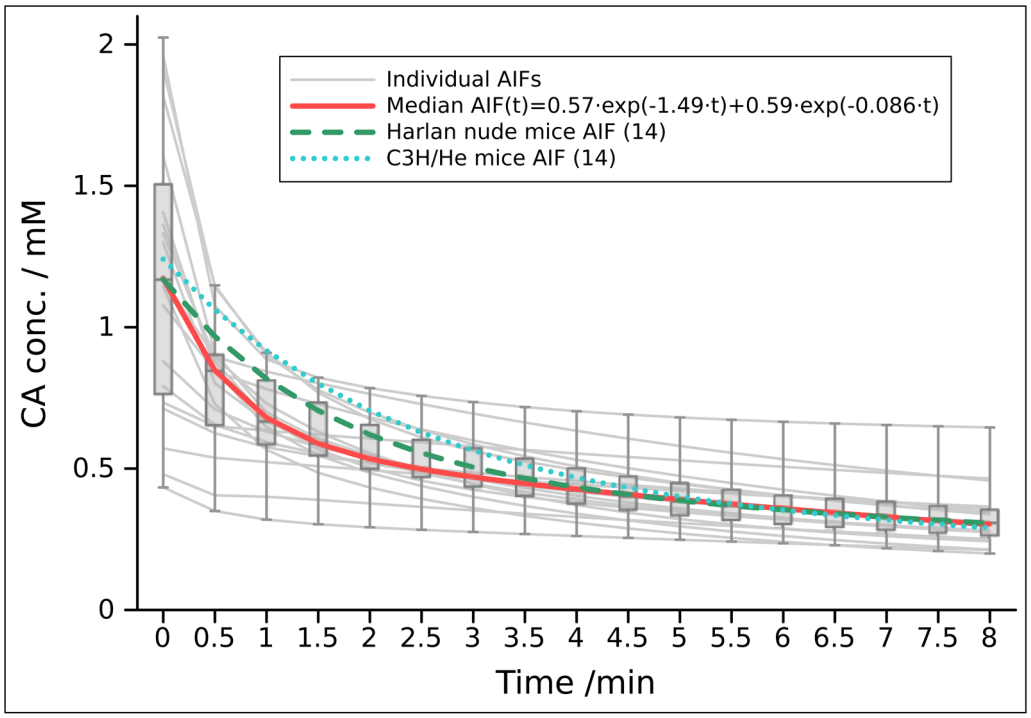

Figure 4.
Individual and median AIF values for the 19 successful experiments for the first 8 min after CA injection. There was a high variation in individual AIF values, especially for the initial values with the median CA concentration of 1.17 mM. A bi-exponetial fitting curve was used for a better comparison with previously reported values of average AIF obtained from Harlan nude mice and C3H/He mice with similar injection parameters (14).

Table 1

Comparison of mean values (±standard deviation) of pharmacokinetic parameters of muscle and tumor regions for the 19 dynamic contrast-enhanced (DCE)-MRI experiments in our study with those from DCE-MRI studies in small rodents[a]

Parameter	K^{trans}/min^{-1}	k_{ep}/min^{-1}	v_e	v_p
Muscle (our study)	0.038 ± 0.025	0.66 ± 0.48	0.060 ± 0.014	0.033 ± 0.021
Muscle (literature)	0.044 ± 0.033[b]	0.55[c]	0.080 ± 0.040[d]	0.028 ± 0.008[e]
Tumor (our study)	0.082 ± 0.071	0.82 ± 0.80	0.121 ± 0.075	0.093 ± 0.051
Tumor [f] (literature)	0.062 ± 0.017	0.41[c]	0.15 ± 0.04	0.04 ± 0.01

[a] References given in parentheses.

[b] K^{trans} is the average value for perivertebral muscle in mice obtained from 2 separate contrast agent injections (16).

[c] k_{ep} was calculated by Eq. 3, using values reported for K^{trans} and v_e in literature (16, 17).

[d] v_e values are for rat skeletal muscle (16).

[e] v_p is the average value obtained from 2 different limb muscles in rabbit (15).

[f] Values for orthotopic BN472 breast tumor xenografts in Brown Norway rat (16).